Long-Range Atmospheric Transport of Polycyclic Aromatic Hydrocarbons: A Global 3-D Model Analysis Including Evaluation of Arctic Sources*

Carey L. Friedman and Noelle E. Selin

GLOBAL CHANGE

MIT JOINT PROGRAM ON THE SCIENCE AND POLICY of GLOBAL CHANGE

The MIT Joint Program on the Science and Policy of Global Change combines cutting-edge scientific research with independent policy analysis to provide a solid foundation for the public and private decisions needed to mitigate and adapt to unavoidable global environmental changes. Being data-driven, the Program uses extensive Earth system and economic data and models to produce quantitative analysis and predictions of the risks of climate change and the challenges of limiting human influence on the environment—essential knowledge for the international dialogue toward a global response to climate change.

To this end, the Program brings together an interdisciplinary group from two established MIT research centers: the Center for Global Change Science (CGCS) and the Center for Energy and Environmental Policy Research (CEEPR). These two centers—along with collaborators from the Marine Biology Laboratory (MBL) at Woods Hole and short- and long-term visitors—provide the united vision needed to solve global challenges.

At the heart of much of the Program's work lies MIT's Integrated Global System Model. Through this integrated model, the Program seeks to: discover new interactions among natural and human climate system components; objectively assess uncertainty in economic and climate projections; critically and quantitatively analyze environmental management and policy proposals; understand complex connections among the many forces that will shape our future; and improve methods to model, monitor and verify greenhouse gas emissions and climatic impacts.

This reprint is one of a series intended to communicate research results and improve public understanding of global environment and energy challenges, thereby contributing to informed debate about climate change and the economic and social implications of policy alternatives.

Ronald G. Prinn and John M. Reilly,
Program Co-Directors

Long-Range Atmospheric Transport of Polycyclic Aromatic Hydrocarbons: A Global 3-D Model Analysis Including Evaluation of Arctic Sources

Carey L. Friedman*,[†] and Noelle E. Selin[‡]

[†]Center for Global Change Science, Massachusetts Institute of Technology, Cambridge, Massachusetts 02139, United States

[‡]Engineering Systems Division and Department of Earth, Atmospheric, and Planetary Sciences, Massachusetts Institute of Technology, Cambridge, Massachusetts 02139, United States

S *Supporting Information*

ABSTRACT: We use the global 3-D chemical transport model GEOS-Chem to simulate long-range atmospheric transport of polycyclic aromatic hydrocarbons (PAHs). To evaluate the model's ability to simulate PAHs with different volatilities, we conduct analyses for phenanthrene (PHE), pyrene (PYR), and benzo[a]pyrene (BaP). GEOS-Chem captures observed seasonal trends with no statistically significant difference between simulated and measured mean annual concentrations. GEOS-Chem also captures variability in observed concentrations at nonurban sites (r = 0.64, 0.72, and 0.74, for PHE, PYR, and BaP). Sensitivity simulations suggest snow/ice scavenging is important for gas-phase PAHs, and on-particle oxidation and temperature-dependency of gas-particle partitioning have greater effects on transport than irreversible partitioning or increased particle concentrations. GEOS-Chem estimates mean atmospheric lifetimes of <1 day for all three PAHs. Though corresponding half-lives are lower than the 2-day screening criterion for international policy action, we simulate concentrations at the high-Arctic station of Spitsbergen within four times observed concentrations with strong correlation (r = 0.70, 0.68, and 0.70 for PHE, PYR, and BaP). European and Russian emissions combined account for ~80% of episodic high-concentration events at Spitsbergen.
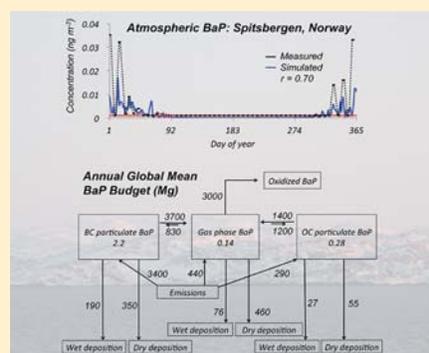
■ INTRODUCTION

Polycyclic aromatic hydrocarbons (PAHs) are contaminants of concern because of their detrimental health effects. PAHs travel through the atmosphere across national boundaries[1] and are found in Arctic regions far from sources[2,3] where they dominate invertebrate and fish persistent organic pollutant (POP) tissue burdens. PAH concentrations are at least 100× higher than other legacy POPs.[4] PAHs are regulated internationally as POPs by the United Nations Economic Commission for Europe's (UNECE's) Convention on Long-Range Transboundary Air Pollution (CLRTAP), but there remains uncertainty surrounding pathways by which they reach remote regions, especially with respect to gas−particle partitioning and oxidation. Here we use the chemical transport model (CTM) GEOS-Chem to investigate the influence of uncertain PAH properties on atmospheric transport and source−receptor relationships globally.

Existing PAH models have over- or underpredicted observed concentrations by ~2× (e.g., in Europe[5]) to more than 10× (e.g., at Arctic locations[6]). Previous investigations of PAH/POP atmospheric transport have relied primarily on two model types: multimedia screening/assessment tools, and regional CTMs. Multimedia models[7−11] focus on pollutant chemical properties while the larger environment has fixed character-

istics, and are commonly used to identify a POP's potential for environmental persistence or long-range transport.[12] Regional CTMs and trajectory models, by contrast, consider dynamic atmospheric processes in addition to pollutant properties and have been used to investigate PAH distribution over Europe,[5,13] cross-Pacific sources to western U.S. receptors,[14] sources to the Arctic,[15] and transboundary outflow.[16−18] Lammel et al.[19] used a general circulation model (GCM) to investigate global transport of anthracene, fluoranthene, and benzo[a]pyrene (BaP). Their simulations demonstrated that gas−particle partitioning has a substantial effect on long-range transport, with a parametrization assuming absorption into organic matter and adsorption to black carbon (BC) agreeing best with remote observations.

Our use of GEOS-Chem to simulate PAHs makes several important contributions to POPs modeling. We use a finer spatial resolution (4° × 5°) than previous global POP models,[20] and thus can conduct a detailed model performance evaluation at multiple sites. The representation of atmospheric oxidants,

partitioning, and deposition at this scale allows us to examine in detail their influence on PAH behavior, similar to studies with regional models[5,13] but providing a global perspective on transport. Additionally, because the model is driven by assimilated meteorology,[21] we can assess the influence of episodic transport to remote locations.

Here we describe model development, compare results to observations, and assess the importance of oxidation, gas–particle partitioning, and deposition to the global atmospheric lifetimes of phenanthrene (PHE), pyrene (PYR), and BaP (three-, four-, and five-benzene ring PAHs, respectively). These PAHs were chosen on the basis of variation in expected fraction associated with particles (with PHE primarily in the gas phase, BaP primarily in the particulate phase, and PYR in both phases), and because of potential toxicity.[22,23] We then use the model to investigate the effect on global concentrations and particulate fraction of (i) temperature-dependent partitioning, (ii) nonreversible partitioning, (iii) increased particle concentrations, (iv) variable gas-phase oxidation, and (v) on-particle oxidation. Additionally, we simulate PAHs in the remote Arctic and attribute concentrations to different source regions.

METHODS

General Model Description. We use GEOS-Chem version 8-03-02[21] (http://www.geos-chem.org/) to simulate gas phase, organic carbon (OC)-bound particulate, and BC-bound particulate PAH global transport and chemistry. The model is driven by GEOS-5 assimilated meteorology from the NASA Goddard Earth Observing System (GEOS) with 6-h temporal resolution, 47 vertical levels, and $0.5° \times 0.667°$ horizontal resolution, regridded to $4° \times 5°$ for input to the PAH simulation. Simulations are conducted for meteorological years 2004–2009, with 2004 used for initialization.

Emissions. We use the 2004 global atmospheric PAH emission inventory from Zhang and Tao.[24] Total (gas + particulate) annual emissions were 6.0×10^4 Mg, 2.1×10^4 Mg, and 4.1×10^3 Mg for PHE, PYR, and BaP, respectively, with no seasonal variation. Biofuel is the dominant source (57%), and Chinese emissions predominate (27%, 30%, and 37% of total for PHE, PYR, and BaP, respectively). Emissions are regridded from $1° \times 1°$ to $4° \times 5°$ horizontal resolution for inclusion in the model. PAHs are emitted as total concentrations and then distributed between the gas and particle phase throughout the planetary boundary layer by considering ambient OC/BC concentrations. We neglect re-emissions from surfaces, as monitoring data suggests PAH concentrations in the ocean surface and atmosphere are unconnected,[25] and quantification of fluxes has been limited. However, as recent studies suggest PAH re-emission from soils may contribute to atmospheric concentrations,[26] inclusion of secondary sources is a priority for further model development.

Gas–Particle Partitioning. An OC absorption model, in which a compound's octanol–air partition coefficient (K_{OA}) describes its sorption into the particle organic fraction,[27,28] is often used to model PAH/POP gas–particle partitioning.[3,29] PAHs have also been shown to strongly adhere to particulate BC.[30] We implement a dual OC absorption and BC adsorption model[30] using both K_{OA}[31] and a BC–air partition coefficient (K_{BC})[32] to describe PAH partitioning in/onto OC and BC aerosols, respectively. We incorporate K_{OA} temperature dependence into the default model according the van't Hoff relationship (see Supporting Information (SI) for details).

The temperature dependency of K_{OA} is well established, but that of K_{BC} as a surface process is less certain, particularly as we use an empirical K_{BC} considering BC volume rather than surface area. Therefore, in our standard model, K_{BC} does not vary with temperature. However, as the temperature dependence of PAH surface adsorption to soot has been shown to follow the van't Hoff relationship,[33] we conduct sensitivity analyses where K_{BC} varies according to the van't Hoff equation (Equation S1 and Table S1).

Monthly mean hydrophobic OC and BC concentrations for all years are from GEOS-Chem aerosol simulations for 2008 using emissions from Bond et al.[34] scaled following Wang et al.[35] (see SI for details). GEOS-Chem assumes 50% of OC and 80% of BC emissions are hydrophobic with lifetimes of 1.2 days before conversion to hydrophilic OC and BC.[36] Empirical and modeling observations suggest this conversion rate should vary regionally and may be too fast.[37,38] Therefore, we also conduct an increased aerosol sensitivity analysis with 2× OC and BC concentrations.

Oxidation. We incorporate PAH loss through reaction with hydroxyl radical (OH). We use an empirically derived rate constant (k_{OH}) for PHE,[39] with sensitivity simulations conducted using a k_{OH} calculated with the U.S. EPA's AOPWIN software.[40] PYR and BaP k_{OH}'s are calculated with AOPWIN. Standard simulations have temperature-independent k_{OH}'s, but a PHE sensitivity analysis was conducted with temperature dependency (see SI text and Table S1).

The importance of on-particle BaP oxidation by ozone (O$_3$), the PAH for which O$_3$ reaction rate constants (k_{O3}) have been most widely determined, was tested with three parametrizations (see SI for details): (i) k_{O3} for BaP on soot particles from Pöschl et al.,[41] (ii) k_{O3} for BaP dissolved in octanol from Kahan et al.,[42] and (iii) k_{O3} for BaP on wet azaelic acid aerosols from Kwamena et al.[43] On-particle oxidation schemes were tested for BC-phase BaP only (for consistency with the Pöschl scheme which only applies to soot) and were not included in standard simulations.

Deposition. Wet deposition includes rainout and washout from large-scale and convective precipitation and scavenging in convective updrafts[44] and is compatible with GEOS-Chem version 9-02-01. Wet deposition is applied to both gas and particulate PAHs. Gas-phase PAHs are scavenged into liquid water according to the temperature-dependent air–water partition coefficient (K_{AW}[31]) and retained at 100% efficiency above 268 K and 0% otherwise. However, as cold-temperature scavenging is likely an important process,[45,46] we also investigate the addition of gas-phase PHE scavenging by ice (i.e., precipitation ≤268 K) using a PHE snow scavenging ratio from Wania et al.[45] Particle-phase PAHs are scavenged as hydrophobic OC and BC aerosols[44] in the default model, with a hydrophilic OC and BC scavenging efficiency tested in a sensitivity analysis.

PAH dry deposition velocities are calculated following a resistance-in-series scheme from Wesely et al.[47] with improvements by Wang et al.[48] We adjust this scheme by scaling cuticular resistances with K_{OA} to account for lipophilic uptake of gas-phase PAHs in waxy leaf cuticles.[49,50] Uptake of particulate PAHs into plant material is not considered, as uptake of gaseous PAHs is the dominant pathway.[51]

Source–Receptor Relationships. We assess the model's ability to reproduce episodic transport to remote sites by simulating daily concentrations for 2005–2009 at the Spitsbergen, Norway, EMEP Arctic monitoring station (80N,

12E). We investigate the contribution of various source regions by removing emissions from source regions designated by the CLRTAP (Europe: 10W−50E, 25N−65N; North America: 125W−60W, 15N−55N; East Asia: 95E−160E, 15N−50N; South Asia: 50E−95E, 5N−35N) and rerunning the 2007 time series. Though not a CLRTAP source region, we also investigate the impact of Russian emissions (50E−180E, 50N−75N) on Spitsbergen.

■ RESULTS AND DISCUSSION

Annual Mean Concentrations. Figure 1 shows global simulated annual mean total (gas + particulate) PHE, PYR, and BaP concentrations for 2005−2009 compared with observations. All observations are from land-based northern hemisphere sites and were collected using high-volume air samplers.
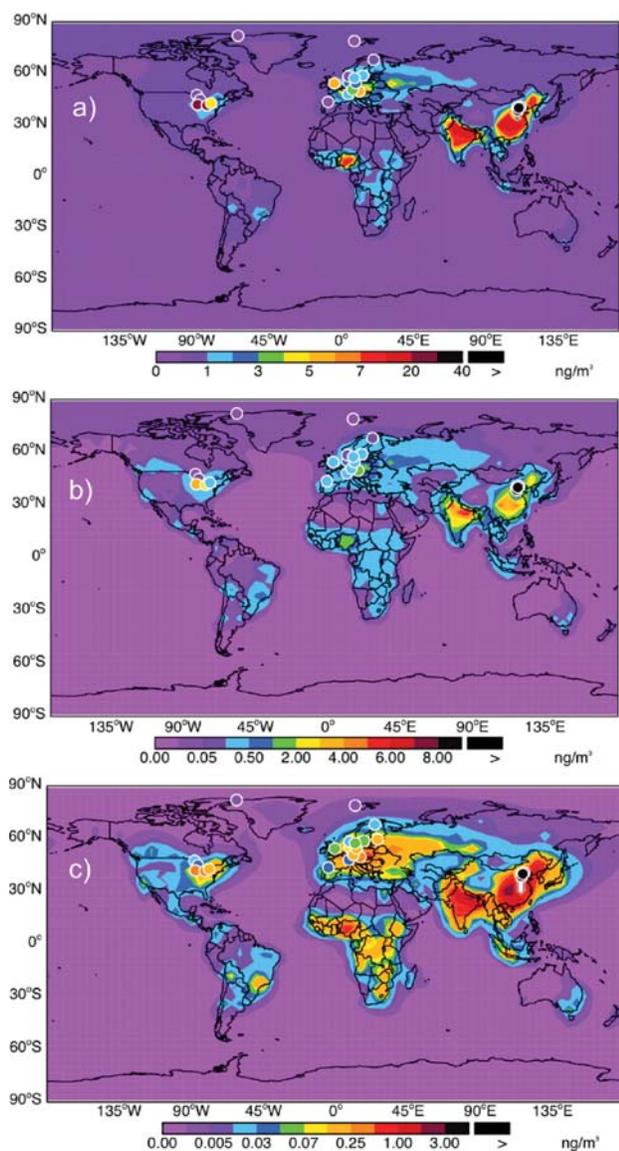

Figure 1. Average PHE (a), PYR (b), and BaP (c) total (gas + particulate) simulated concentrations in surface air from 2005 to 2009 (background). Land-based observations from Table 1 are shown with circles. Observations from long-term monitoring stations are interannual means for the years shown in Table 1.

Table 1 shows mean annual total concentrations observed and simulated at each location. Also shown are total observed and simulated means from all sites, from nonurban locations only, and from Arctic locations only.

The GEOS-Chem simulation successfully reproduces the five-year mean concentrations overall and captures variability among nonurban sites. Differences between mean observed and simulated concentrations from all sites ($n = 19$ for PHE and PYR and $n = 20$ for BaP after averaging observations within the same grid box) are not statistically significant at $\alpha = 0.05$ ($p = 0.10$, 0.17, and 0.41 for PHE, PYR, and BaP, respectively), though high variability in observed concentrations contributes to this indifference. When only nonurban sites are considered ($n = 15$ for PHE and PYR, $n = 16$ for BaP), discrepancies between observed and simulated concentrations decrease for all three compounds, but because variance also decreases, differences become statistically significant for PYR and BaP (Table 1; $p = 0.27$, 0.04, and <0.01 for PHE, PYR, and BaP, respectively). However, there is a significant correlation (r) between simulated and measured concentrations at nonurban sites (0.64 (PHE), 0.72 (PYR), and 0.74 (BaP), with $p < 0.01$ for all three; Figure S1). Mean simulated Arctic concentrations generally match observations well, though too few observations are available for statistical analyses.

We compared mean annual concentrations to ship-based measurements from the Atlantic[52,53] (data not shown). Simulated concentrations were generally >10× lower than measured, likely because of (i) omission of secondary emissions from oceans, (ii) interference in cruise-based measurements from ship stack vapors, which can lead to strong overestimates,[25] or (iii) lack of seasonality in emissions.

Seasonal Variation. We compare seasonal variation in simulated and observed total PAH concentrations at all nonurban midlatitude (NUML) and Arctic sites from Table 1 to assess the influence of natural seasonal processes (Figures 2 and 3, and Figures S2 and S3). For all three PAHs, mean observed concentrations over NUML and Arctic sites are significantly higher in winter than in summer at most locations ($p < 0.005$),[15,54,55] reflecting the influence of oxidative loss, gas−particle partitioning, and seasonal variation in emissions. GEOS-Chem captures this seasonal variability ($p \ll 0.001$) despite using a constant emission rate.

At NUML sites (Figure 2), GEOS-Chem simulates monthly mean PHE and PYR within one standard deviation of measured means, but overestimates BaP. GEOS-Chem systematically overestimates winter concentrations for all three PAHs. We explore the influence of oxidation on this overestimate below.

Arctic concentrations exhibit stronger seasonal variation than NUML sites (Figure 3), reflecting either increased seasonal variation in oxidation or transport, or the effect of springtime Arctic haze.[56] Wintertime concentrations are ∼3×, 6×, and 8× higher than summer in observations. GEOS-Chem overestimates winter PHE concentrations by ∼4×, and underestimates summer concentrations. The model exhibits a smaller overestimate of Arctic winter PYR, and no bias in BaP, suggesting it does not capture a gas-phase natural process or underestimates the particulate fraction (f_P, equal to the sum of OC- and BC-phase PAH divided by the sum of the gas-, OC-, and BC-phases, discussed further below), as the bias decreases with increasing particle partitioning. To test whether snow/ice scavenging is responsible for the discrepancy, we conducted a simulation including wet scavenging of gas-phase PHE at temperatures below 268 K. Results for Arctic stations (Figure

9503

dx.doi.org/10.1021/es301904d | Environ. Sci. Technol. 2012, 46, 9501−9510

Table 1. Mean (±1 Standard Deviation) Total (Gas + Particulate) Concentrations Observed and Simulated at Measurement Locations (2005–2009)

lat	long.	location name	observation years	ref	mean total concentration (ng m⁻³)					
					PHE obsd	PHE simulated	PYR observed	PYR simulated	BaP obsd	BaP simulated
82	−62	Alert, Canada	2004–2008	1	0.065	0.138	0.025	0.016	0.002	0.000
80	12	Spitsbergen/Zeppelinfjell, Norway	2004–2009	2	0.063	0.260	0.018	0.035	0.003	0.002
68	24	Pallas/Matorova, Finland[c]	2004–2007	2	0.405	0.688	0.079	0.118	0.020	0.014
60	26	Lahemaa, Estonia	2007–2008	2	NA	2.115	NA	0.394	0.133	0.156
60	17	Aspvreten, Sweden[c]	2004–2008	2	1.261	2.279	0.238	0.483	0.056	0.135
58	8	Birkenes, Norway	2008–2009	2	0.767	2.279	0.093	0.483	0.024	0.167
57	12	Rao, Sweden[c]	2004–2008	2	1.085	3.083	0.249	0.600	0.062	0.167
55	8	Westerland, Germany	2007–2008	2	2.455	3.057	0.535	0.646	0.081	0.264
54	13	Zingst, Germany	2006–2008	2	2.802	1.328	0.365	0.255	0.108	0.293
54	−1	High Muffles, Great Britain	2004–2008	2	5.282	5.614	0.443	1.142	0.055	0.106
51	11	Schmucke, Germany	2007–2008	2	3.306	5.347	0.424	1.187	0.094	0.474
50	15	Kosetice, Czech Republic	2004–2008	2	5.630	4.688	1.226	1.010	0.305	0.547
48	8	Schauinsland, Germany	2007–2008	2	1.468	0.138	0.207	0.016	0.042	0.423
47	−88	Eagle Harbor, MI[a]	2004–2008	3	0.403	0.609	0.047	0.099	0.011	0.032
45	−86	Sleeping Bear Dunes, MI[a]	2004–2008	3	0.600	0.651	0.098	0.104	0.033	0.032
43	−5	Niembro, Spain	2004–2006	2	0.024	0.762	0.178	0.158	0.031	0.059
43	−79	*Sturgeon Point, NY[a]*	2004–2008	3	*4.787*	*3.606*	*0.499*	*0.761*	*0.095*	*0.239*
42	−88	*Chicago, IL[a,b]*	2004–2008	3	*28.037*	*2.240*	*3.024*	*0.416*	*0.408*	*0.130*
41	−82	*Cleveland, OH[a,b]*	2004–2008	3	*28.611*	*3.606*	*2.911*	*0.761*	*0.319*	*0.239*
41	117	Gubeikou, China[a,b]	2007–2008	4	68.825	2.869	18.475	0.816	3.425	0.436
40	116	**Beijing, China[a,b]**	**2007–2008**	4	**92.125**	**21.353**	**14.625**	**6.637**	**4.150**	**2.975**
40	115	XiaoLongmen, China[a,b]	2007–2008	4	10.500	21.353	0.750	6.637	0.167	2.975
39	116	Donghe, China[a,b]	2007–2008	4	217.825	21.353	35.525	6.637	9.075	2.975
mean from all locations ±1 sd					12.9 ± 28.0	3.31 ± 4.67	2.34 ± 5.46	0.81 ± 1.46	0.48 ± 1.20	0.34 ± 0.65
mean from nonurban locations ±1 sd					1.71 ± 1.83	2.19 ± 1.84	0.28 ± 0.31	0.45 ± 0.40	0.07 ± 0.07	0.18 ± 0.18
mean from Arctic locations ±1 sd					0.178 ± 0.197	0.362 ± 0.289	0.040 ± 0.034	0.057 ± 0.054	0.008 ± 0.010	0.006 ± 0.008

[a]Gas−particle ratios provided by reference. [b]Site considered urban and/or highly impacted by local sources. Sites >66°N are considered Arctic. [c]Mean seasonal total deposition (wet + dry) provided by reference. Observations from sites formatted similarly (italics or bold, e.g.,) occurred within the same GEOS-Chem grid box and were averaged. References: (1) Northern Contaminants Program and Environment Canada; (2) EMEP; (3) IADN; (4) Wang et al. (2011).[66] Data from ref 3 was provided prior to a routine QA/QC procedure.
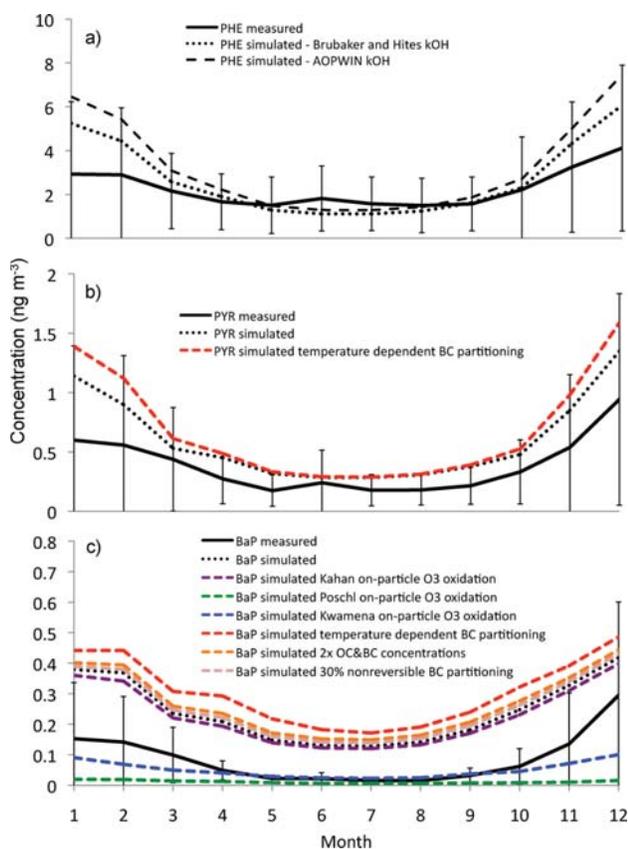
Figure 2. Nonurban midlatitude mean total concentration (gas + particle) seasonal variation from sites/years listed in Table 1 (solid black line) and for simulated years 2005−2009 (dotted black line) for (a) PHE, (b) PYR, and (c) BaP. Error bars are ±1 standard deviation of monthly means across sites. Colored lines represent results from sensitivity analyses.

Figure 3. Arctic mean total concentration (gas + particle) seasonal variation from sites/years listed in Table 1 (solid black line) and for simulated years 2005−2009 (dotted black line) for (a) PHE, (b) PYR, and (c) BaP. Error bars are ±1 standard deviation of monthly means across sites. Colored lines represent results from sensitivity analyses.

3a) suggest cold-temperature scavenging can reduce winter simulated gas-phase concentrations by up to 30%, but will not account for the full disagreement. Daly and Wania[46] suggested scavenging by the snowpack on land may contribute to reduced atmospheric concentrations; this could further reduce Arctic wintertime PHE. A wide range of observed particle-phase snow scavenging ratios[46] suggests snow could also have a non-negligible effect on BaP concentrations.

In contrast to NUML and Arctic sites, Great Lakes (U.S.) and urban locations show a maximum in summer, particularly for PHE, which GEOS-Chem does not capture (Figure S4). The summer maximum may be due to volatilization of higher vapor pressure PAHs from polluted land/water surfaces during warmer temperatures, a process not included in our simulation. Given that the model captures observed NUML seasonal trends without including emissions variability, the trends are likely due primarily to natural processes.

Global Budget. Figure S5 shows mean annual global budgets of gas-, OC-, and BC-phase PHE, PYR, and BaP in GEOS-Chem for 2005−2009, and Table S2 shows simulated lifetimes with respect to different removal processes, the overall lifetime of each PAH in each phase, and total (gas + particulate) lifetimes. Overall lifetimes are 4, 3, and 6 h and the mean f_P's are 0.002, 0.02, and 0.93, for PHE, PYR, and BaP, respectively. Overall lifetimes are shorter than those predicted by other modeling studies, especially for BaP, which is almost
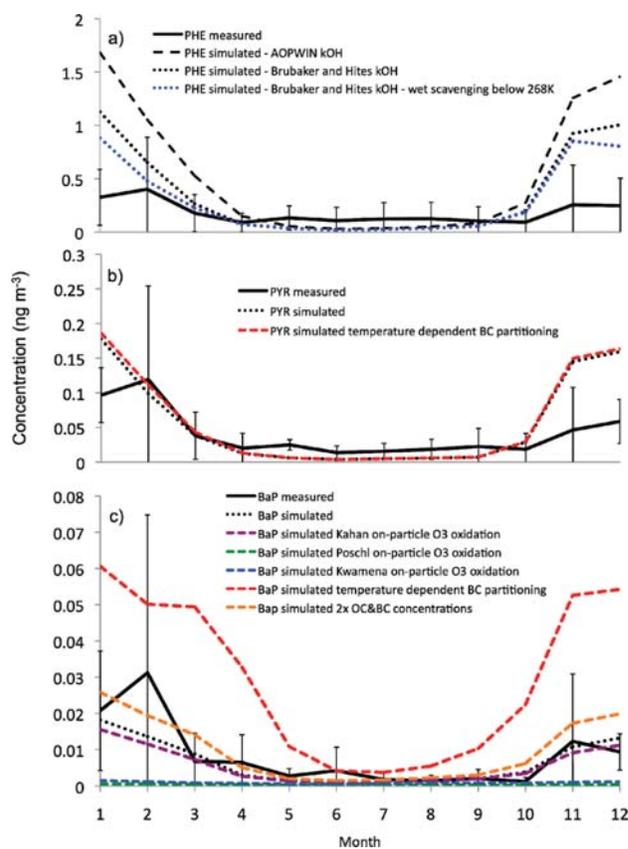
completely in the particle phase; e.g., Lammel et al.[19] report a BaP lifetime of 48 h.

We find that as PAH molecular weight (and f_P) increases, overall lifetimes stay fairly consistent. Similar lifetimes result from three concurrent processes: (i) decreasing gas-phase lifetimes balancing an increasing f_P, (ii) low variability between OC and BC deposition lifetimes for different PAHs, and (iii) exchange between the gas and OC/BC phases dominating over deposition with consistent net exchange across PAHs (Figure S5). Gas-phase lifetimes with respect to oxidation are ~4, 3, and 0.4 h for PHE, PYR, and BaP, respectively. The PHE oxidation lifetime is in the same range as that found by Halsall et al.[3] for summertime transport from the U.K. to the Arctic. Despite the same k_{OH}'s, BaP oxidation lifetime is ~10× shorter than that of PYR. Spatial and temporal differences in gas phase prevalence account for this: BaP exists as a gas only in warmer regions and seasons where OH concentrations tend to be higher. Gas-phase lifetimes with respect to wet and dry deposition decrease with increasing PAH molecular weight, owing to decreasing K_{AW}'s and increasing K_{OA}'s, respectively. OC- and BC-phase lifetimes do not vary substantially between PAHs, so increases in the particulate phase result in greater deposition. Despite a shorter lifetime and a similar gas−particle partitioning parametrization, GEOS-Chem predicts higher BaP concentrations in remote regions than the global model of Lammel et al.[19] Greater BaP emissions and potentially longer aerosol lifetimes are likely causes of the discrepancy.

Gas−Particle Partitioning. To evaluate the effect of gas−particle partitioning on global concentrations, we compare monthly mean simulated PAH f_Ps to those from the Integrated Atmospheric Deposition Network (IADN; Table 1), and conduct sensitivity simulations using different partitioning parametrizations (Figure 4). On average, our standard model
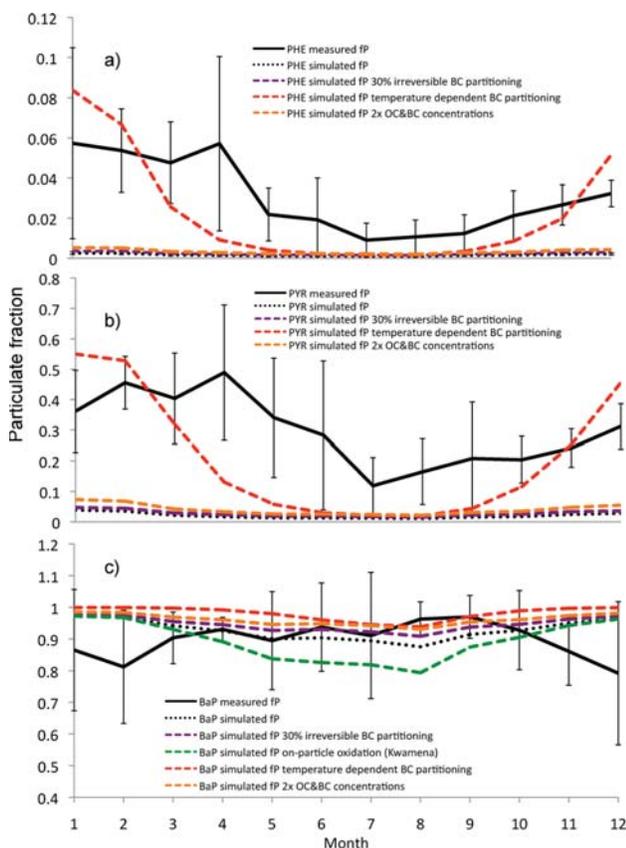

Figure 4. Mean particulate fraction measured (solid black line) at IADN sites over years 2004−2008 and mean simulated particulate fraction (dotted black line) at same sites for years 2005−2009. Error bars represent one standard deviation of monthly mean particulate fraction across sites. Colored lines represent results from sensitivity analyses.

simulates observed f_P for BaP well (0.93 annual mean, compared with 0.90 in measurements), but underpredicts observed f_P for PHE and PYR by ∼10×. The IADN, covering sites near the U.S. Great Lakes, provides the most consistent f_P data, but comparisons should be interpreted with caution because (i) data from 2005 onward have not yet undergone quality assurance/control procedures (M. Venier, Indiana University, personal communication), and (ii) half of IADN's sites are urban, and gas−particle partitioning may depend strongly on the distribution upon emission. Though f_P has been measured at high latitude stations, we do not consider them here because long sampling periods with high flow rates can cause biases toward the gas phase (H. Hung, Environment Canada, personal communication).

We examine three hypotheses for low simulated PHE and PYR f_P and conduct sensitivity simulations to test the effect of including these processes on both f_P and total concentrations. First, partitioning between gas and particles is likely not 100% reversible: Galarneau et al.[57] and Arp et al.[58] observed f_P's

orders of magnitude higher than predicted and attributed them to a fraction of particulate PAH that is analytically extractable but nonexchangeable with the gas phase. Second, simulated OC and BC concentrations could be too low, or the hydrophobic to hydrophilic folding time could be too fast.[37,38] Third, sorption to BC is likely temperature-dependent.[33,59]

To test the effect of irreversible partitioning, we assume 30% of BC-associated PAH becomes trapped within the particle volume while 70% is available for surficial reversible partitioning (given BC's high surface area[41]). This results in a small increase in the mean f_P (Figure 4), not enough to match measured f_P, a minor increase in the total concentrations (Figure 2c), and negligible increases in total atmospheric burdens.

To test the influence of increased OC and BC, we double OC and BC concentrations globally. This increases f_P only slightly (Figure 4), and has a negligible effect on NUML concentrations for PHE and PYR (data not shown). BaP NUML concentrations increase on average by 1.1× (Figure 2c), amplifying their positive bias, and Arctic BaP concentrations increase by 1.5× (Figure 3c). Increasing OC and BC concentrations does not substantially affect the overall lifetime or atmospheric burdens of PHE or PYR, but increases BaP's lifetime by ∼1 h and global burden by 1.1×.

To test the effect of temperature-dependent BC partitioning, we include a K_{BC} that follows the van't Hoff equation. This increases f_P for all compounds such that PHE and PYR simulated f_P values are now within the range of observed f_P (Figure 4). PHE and PYR f_P increase by an order of magnitude, but BaP increases by only 1.1×. Making K_{BC} temperature-dependent does not affect total NUML concentrations of PHE (data not shown), but slightly increases those of PYR (by 1.1 ×) and BaP (by 1.3×; Figure 2b,c), increasing their positive bias. It also increases PYR and BaP concentrations in the Arctic (by 1.1× and 4.9×, respectively; Figure 3b,c), and the atmospheric burden of each (by 1.1× and 1.3×, respectively). We conclude that temperature-dependent BC partitioning is the most likely explanation for the f_P underprediction; this suggests BC temperature-dependent partitioning may be reasonably approximated by considering BC volume rather than surface area.

Oxidation. We test several different oxidation schemes for individual PAHs: (i) temperature dependence for PHE; (ii) the magnitude of k_{OH} for PHE; and (iii) on-particle oxidation for BaP.

Including temperature dependence in k_{OH} for PHE does not affect mean NUML concentrations (data not shown), consistent with the near-zero activation energy for PHE.[39] Using the AOPWIN PHE k_{OH}, which is ∼half our default k_{OH}, increases average seasonal concentrations and the atmospheric burden (both by 1.2×), with a stronger effect in winter (Figure 2a). The AOPWIN k_{OH} also increases mean Arctic concentrations (by 1.5×; Figure 3a), decreasing measurement-model agreement. Results suggest k_{OH}'s may be underestimated and/or other oxidants play a non-negligible role in gas-phase PAH removal. Both k_{OH} sensitivity analyses affect PHE f_P by less than 0.1% (data not shown).

We test the three different parametrizations for reaction of O_3 with on-particle BaP described in the Methods section and SI. The effect on total BaP concentrations depends strongly on the O_3 reaction scheme used. Experimental studies have shown that PAHs can be rapidly oxidized by O_3 at the particle surface,[41−43] but models often omit this process. Matthias et al.[5] included O_3 oxidation of BaP in European regional modeling experiments and found that it decreased simulated

concentrations by 5×, bringing simulated and measured concentrations closer. When we apply the Pöschl scheme, NUML and Arctic BaP concentrations are reduced >30× and the total atmospheric burden by 18×, causing large underestimates of observed concentrations (Figures 2c and 3c). The Kahan scheme does not substantially reduce concentrations for either the NUML stations or Arctic stations, and reduces the atmospheric burden by only 10%. At NUML sites, the Kwamena scheme reduces average concentrations by 5× (Figure 2c), improving the match to observations, similar to Matthias et al.,[5] who also used the Kwamena scheme. The total atmospheric burden is also reduced by 5×. In the Arctic, however, concentrations are reduced by 11×, weakening the match to observations and reducing seasonal variation. In general, the Kwamena scheme brings observed and simulated concentrations closest together, and has little effect on the BaP f_P, which is already well-simulated. We conclude that on-particle oxidation has a substantial effect on BaP concentrations, and that a rate intermediate to the Kahan and Kwamena schemes best matches existing data constraints. There remains considerable uncertainty in on-particle oxidation rates, which depend on particle content and size, relative humidity, and ambient temperature.

Deposition. Deposition flux measurements are available at few sites, and all are in northern Europe ($n = 3$, Table 1). We compare mean simulated seasonal and annual combined wet and dry deposition fluxes to observed (ng m^{-2} day^{-1}; Figures S6–S8). Similar to other models,[5] ours overestimates deposition at these sites by ~5.6×, with better agreement in the winter for PHE and PYR. Some of this difference may be explained by overprediction of concentrations at those sites, which are all in the same region, or by not accounting for emissions seasonality. Additionally, we may underestimate oxidative losses as sensitivity analyses indicated. The limited number of sites, however, provides few constraints; additional deposition measurements would improve our ability to constrain the relative magnitudes of emission, deposition, and oxidation.

Source−Receptor Relationships for Remote Regions. To assess the model's ability to reproduce episodic transport to remote sites, we simulate daily concentrations for 2005−2009 at Spitsbergen, Norway, the Arctic station with the shortest measurement integration time. For 2005 and 2007−2009, correlation ranges are $r = 0.53−0.76$ (PHE), $0.40−0.68$ (PYR), and $0.40−0.70$ (BaP). Figure 5 shows results for 2007. The model captures wintertime variability for all three compounds and reproduces several episodic transport events. While summer concentrations appear underestimated, simulated values are below the quantification limit (W. Aas, European Monitoring and Evaluation Programme, personal communication) and should be interpreted with caution. The model overestimates winter PHE concentrations by ~4×, is nearly 1:1 with measured PYR, and underestimates BaP by ~2×. All other years show similar biases (Figures S9−S12), except 2006, during which anomalously high PYR and BaP concentrations were measured in mid-May; the model does not capture these, which are likely due to local sources, regional fires,[60] or interannual variability in emissions. In general, however, it is unlikely Spitsbergen concentrations have a strong local signal, given the remoteness of the station.[61] We also conduct Spitsbergen simulations at a finer spatial resolution ($2° × 2.5°$) to investigate effects on Arctic transport (Figures S11 and S12);
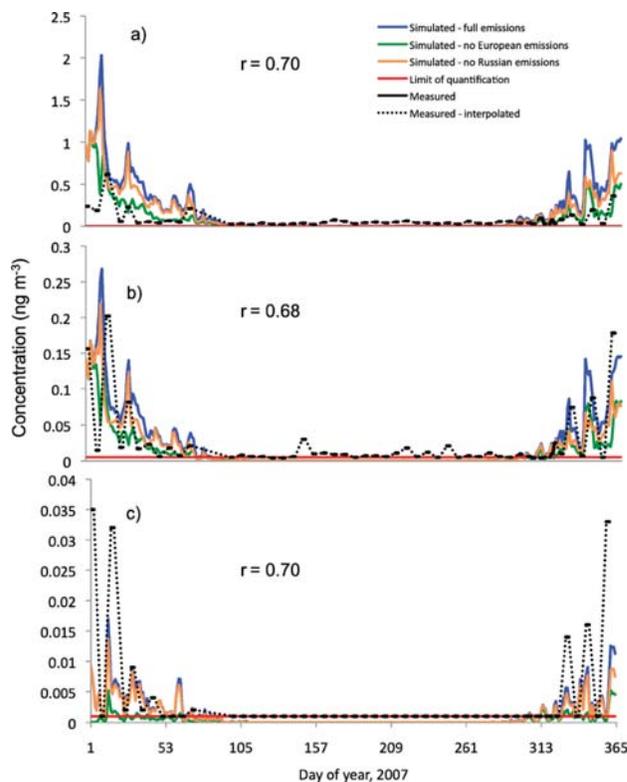

Figure 5. 2007 simulated and measured total (a) PHE, (b) PYR, and (c) BaP at Spitsbergen, Norway. PAHs were measured over three-day periods weekly. Also shown are simulated concentrations when European and Russian emissions are removed from the simulation.

higher concentrations suggest coarser resolutions may average PAH plumes.

We assess the contribution of different regions to Spitsbergen PAH concentrations by removing emissions from source regions designated by the CLRTAP and rerunning the 2007 time series. European emissions contributed the most (51%, 47%, and 70% for PHE, PYR, and BaP, respectively) followed by Russian (24%, 29%, and 13%) and North American (15%, 13%, and 9%). East and South Asian emissions combined contributed 1% (PYR) to 8% (BaP). Most episodic high concentration events can be attributed to European sources (Figure 5).

Though we underestimate mean Spitsbergen BaP by ~2×, this bias compares well to previous efforts to simulate BaP at the same station. Sehili and Lammel[6] modeled the contribution of European and Russian BaP emissions for the years 1994−2004 with a GCM and predicted concentrations as much as 100× less than observed, potentially due to low BaP emissions. Lammel et al.[19] considered global BaP emissions using the same GCM to simulate concentrations at Spitsbergen; this improved agreement with mean concentrations, but winter concentrations were still ~100× lower than observed.

Recommendations for Policy and Measurement Constraints. GEOS-Chem simulates mean global concentrations that are not statistically different from measured, and captures variability in nonurban observations. PAHs have shorter lifetimes in GEOS-Chem than in other models[3,19] with little variation between different PAHs. Discrepancies likely arise from differences in model resolutions and averaging across seasons. Additionally, emissions from wildfires may contribute

to longer PAH lifetimes than accounted for here, since smoke plumes can rise into the free troposphere where constituents are less susceptible to deposition.[62,63] The uncertainty associated with wildfire plumes is likely less than that from lack of seasonality in all emissions sources, however, given that total PAH concentrations vary orders of magnitude between seasons.[15,64]

Lifetimes presented here are >10× less than the threshold for inclusion as a POP under the CLRTAP protocol.[65] Successful simulation of Arctic concentrations, however, suggests model results have a role in hemispheric policy discussions, particularly with respect to prioritizing emissions reductions. Use of the model for more localized policy analysis would benefit from greater spatial and temporal resolution of PAH processes.

The model holds promise for investigating the transport of other semivolatile POPs with similar behaviors, especially when evaluating response of transport to variable particle concentrations, temperature, and oxidizing species. However, there remain substantial uncertainties in physicochemical properties that could have significant impacts on results. Though we find strong dependence of PAH long-range transport on the temperature sensitivity of partitioning and on-particle oxidation, enthalpies of phase exchange and reaction rate constants that govern these processes have not been extensively defined. Combined with international policy interest in aerosols, this suggests the need for improved characterization of these properties. Our modeling highlights areas where land-atmosphere exchange and snow scavenging in the atmosphere and by the snowpack play important roles, but few data exist to constrain efficiencies of these processes. Additionally, over-estimates of deposition suggest a need for alternative sinks in the model and/or additional observational constraints. Finally, measurement networks in Asia, the southern hemisphere, and the Arctic are needed to improve our ability to evaluate PAH fate globally.

ASSOCIATED CONTENT

S **Supporting Information**

Details related to physicochemical constants, oxidation, temperature dependence of gas–particle partitioning, deposition, global budgets, urban concentrations, and Spitsbergen simulations for years 2005, 2006, 2008, and 2009. This material is available free of charge via the Internet at http://pubs.acs.org.

AUTHOR INFORMATION

Corresponding Author
*E-mail: clf@mit.edu.

Notes
The authors declare no competing financial interest.

ACKNOWLEDGMENTS

REFERENCES

(1) NRC. *Global Sources of Local Pollution: An Assessment of Long-Range Transport of Key Air Pollutants to and from the United States*; National Academy of Sciences: Washington, DC, 2009.

(2) Halsall, C. J.; Barrie, L. A.; Fellin, P.; Muir, D. G. C.; Billeck, B. N.; Lockhart, L.; Rovinsky, F.; Kononov, E.; Pastukhov, B. Spatial and temporal variation of polycyclic aromatic hydrocarbons in the Arctic atmosphere. *Environ. Sci. Technol.* **1997**, *31*, 3593−3599.

(3) Halsall, C. J.; Sweetman, A. J.; Barrie, L. A.; Jones, K. C. Modelling the behaviour of PAHs during atmospheric transport from the UK to the Arctic. *Atmos. Environ.* **2001**, *35*, 255−267.

(4) De Laender, F.; Hammer, J.; Hendriks, A. J.; Soetaert, K.; Janssen, C. R. Combining monitoring data and modeling identifies PAHs as emerging contaminants in the Arctic. *Environ. Sci. Technol.* **2011**, *45*, 9024−9029.

(5) Matthias, V.; Aulinger, A.; Quante, M. CMAQ simulations of the benzo(a)pyrene distribution over Europe for 2000 and 2001. *Atmos. Environ.* **2009**, *43*, 4078−4086.

(6) Sehili, A. M.; Lammel, G. Global fate and distribution of polycyclic aromatic hydrocarbons emitted from Europe and Russia. *Atmos. Environ.* **2007**, *41*, 8301−8315.

(7) Scheringer, M. Persistence and spatial range as endpoints of an exposure-based assessment of organic chemicals. *Environ. Sci. Technol.* **1996**, *30*, 1652−1659.

(8) Scheringer, M.; Held, H.; Stroebe, M. *Chemrange 2.1—A Multimedia Transport Model for Calculating Persistence and Spatial Range of Organic Chemicals*; ETH Zürich, Zürich, 2002; http://www.sust-chem.ethz.ch/research/groups/prod_assessment/Projects/chemrange.

(9) Wania, F.; Mackay, D. A global distribution model for persistent organic chemicals. *Sci. Total Environ.* **1995**, *161*, 211−232.

(10) Den Hollander, H.; Van Eijkeren, J. C. H.; Van de Meent, D. *Simplebox 3.0: Multi-Media Mass Balance Model for Evaluating the Fate of Chemicals in the Environment. RIVM 601200003*; National Institute of Public Health and the Environment: Bilthoven, The Netherlands, 2004.

(11) Scheringer, M.; Wegmann, F.; Fenner, K.; Hungerbühler, K. Investigation of the cold condensation of persistent organic pollutants with a global multimedia fate model. *Environ. Sci. Technol.* **2000**, *34*, 1842−1850.

(12) MacLeod, M.; Scheringer, M.; McKone, T. E.; Hungerbühler, K. The state of multimedia mass-balance modeling in environmental science and decision-making. *Environ. Sci. Technol.* **2010**, *44*, 8360−8364.

(13) Aulinger, A.; Matthias, V.; Quante, M. Introducing a partitioning mechanism for PAHs into the Community Multiscale Air Quality modeling system and its application to simulating the transport of benzo(a)pyrene over Europe. *J. Appl. Meteorol. Climatol.* **2007**, *46*, 1718−1730.

(14) Genualdi, S. A.; Killin, R. K.; Woods, J.; Wilson, G.; Schmedding, D.; Massey Simonich, S. L. Trans-Pacific and regional atmospheric transport of polycyclic aromatic hydrocarbons and pesticides in biomass burning emissions to western North America. *Environ. Sci. Technol.* **2009**, *43*, 1061−1066.

(15) Wang, R.; Tao, S.; Wang, B.; Yang, Y.; Lang, C.; Zhang, Y.; Hu, J.; Ma, J.; Hung, H. Sources and pathways of polycyclic aromatic hydrocarbons transported to Alert, the Canadian High Arctic. *Environ. Sci. Technol.* **2010**, *44*, 1017−1022.

(16) Lang, C.; Tao, S.; Liu, W.; Zhang, Y.; Simonich, S. Atmospheric transport and outflow of polycyclic aromatic hydrocarbons from China. *Environ. Sci. Technol.* **2008**, *42*, 5196−5201.

(17) Zhang, Y.; Shen, H.; Tao, S.; Ma, J. Modeling the atmospheric transport and outflow of polycyclic aromatic hydrocarbons emitted from China. *Atmos. Environ.* **2011**, *45*, 2820−2827.

(18) Zhang, Y.; Tao, S.; Ma, J.; Simonich, S. Transpacific transport of benzo[a]pyrene emitted from Asia: Importance of warm conveyor belt

and interannual variations. *Atmos. Chem. Phys.* **2011**, *11*, 11993−12006.

(19) Lammel, G.; Sehili, A. M.; Bond, T. C.; Feichter, J.; Grassl, H. Gas/particle partioning and global distribution of polycyclic aromatic hydrocarbons—A modelling approach. *Chemosphere* **2009**, *76*, 98−106.

(20) MacLeod, M.; Riley, W. J.; McKone, T. E. Assessing the influence of climate variability on atmospheric concentrations of polychlorinated biphenyls using a global-scale mass balance model (BETR-Global). *Environ. Sci. Technol.* **2005**, *39*, 6749−6756.

(21) Bey, I.; Jacob, D. J.; Yantosca, R. M.; Logan, J. A.; Field, B.; Fiore, A. M.; Li, Q.; Liu, H. X.; Mickley, L. J.; Schultz, M. Global modeling of tropospheric chemistry with assimilated meteorology: Model description and evaluation. *J. Geophys. Res.* **2001**, *106*, 23,073−23,096.

(22) U.S. Environmental Protection Agency. *Integrated Risk Information System (IRIS). Benzo[a]pyrene (CASRN 50−32−8)*; http://www.epa.gove/iris/subst/0136.htm.

(23) MacLeod, M.; McKone, T. E.; Foster, K. L.; Maddalena, R. L.; Parkerton, T. F.; Mackay, D. Applications of contaminant fate and bioaccumulation models in assessing ecological risks of chemicals: A case study for gasoline hydrocarbons. *Environ. Sci. Technol.* **2004**, *38*, 6225−6233.

(24) Zhang, Y.; Tao, S. Global atmospheric emission inventory of polycyclic aromatic hydrocarbons (PAHs) for 2004. *Atmos. Environ.* **2009**, *43*, 812−819.

(25) Lohmann, R.; Gioia, R.; Jones, K. C.; Nizzetto, L.; Temme, C.; Xie, Z.; Schulz-Bull, D.; Hand, I.; Morgan, E.; Jantunen, L. Organochlorine pesticides and PAHs in the surface water and atmosphere of the North Atlantic and Arctic Ocean. *Environ. Sci. Technol.* **2009**, *45*, 5633−5639.

(26) Cabrerizo, A.; Dachs, J.; Moeckel, C.; Ojeda, M.-J.; Caballero, G.; Barceló, D.; Jones, K. C. Ubiquitous net volatilization of polycyclic aromatic hydrocarbons from soils and parameters influencing their soil-air partition. *Environ. Sci. Technol.* **2011**, *45*, 4740−4747.

(27) Pankow, J. F. An absorption-model of gas-particle partitioning of organic compounds in the atmosphere. *Atmos. Environ.* **1994**, *28*, 185−188.

(28) Harner, T.; Bidleman, T. F. Octanol-air partition coefficient for describing particle/gas partitioning of aromatic compounds in urban air. *Environ. Sci. Technol.* **1998**, *32*, 1494−1502.

(29) Scheringer, M.; Salzmann, M.; Stroebe, M.; Wegmann, F.; Fenner, K.; Hungerbuhler, K. Long-range transport and global fractionation of POPs: insights from multimedia modeling studies. *Environ. Pollut.* **2004**, *128*, 177−188.

(30) Dachs, J.; Eisenreich, S. J. Adsorption onto aerosol soot carbon dominates gas-particle partitioning of polycyclic aromatic hydro-carbons. *Environ. Sci. Technol.* **2000**, *34*, 3690−3697.

(31) Ma, Y.-G.; Lei, Y.; Xiao, H.; Wania, F.; Wang, W.-H. Critical review and recommended values for the physical-chemical property data of 15 polycyclic aromatic hydrocarbons at 25 °C. *J. Chem. Eng. Data* **2010**, *55*, 819−825.

(32) Lohmann, R.; Lammel, G. Adsorptive and absorptive contributions to the gas-particle partitioning of polycyclic aromatic hydrocarbons: State of knowledge and recommended parametrization for modeling. *Environ. Sci. Technol.* **2004**, *38*, 3793−3803.

(33) Goss, K. U.; Schwarzenbach, R. P. Empirical prediction of heats of vaporization and heats of adsorption of organic compounds. *Environ. Sci. Technol.* **1999**, *33*, 3390−3393.

(34) Bond, T. C.; Bhardwaj, E.; Dong, R.; Jogani, R.; Jung, S.; Roden, C.; Streets, D. G.; Trautmann, N. M. Historical emissions of black and organic carbon aerosol from energy-related combustion, 1850−2000. *Global Biogeochem. Cycles* **2007**, *21*, GB2018.

(35) Wang, Q.; Jacob, D. J.; Fisher, J. A.; Mao, J.; Leibensperger, E. M.; Carouge, C. C.; Le Sager, P.; Kondo, Y.; Jimenez, J. L.; Cubison, M. J.; Doherty, S. J. Sources of carbonaceous aerosols and deposited black carbon in the Arctic in winter-spring: implications for radiative forcing. *Atmos. Chem. Phys.* **2011**, *11*, 12453−12473.

(36) Park, R. J.; Jacob, D. J.; Chin, M.; Martin, R. V. Sources of carbonaceous aerosols over the United States and implications for natural visibility. *J. Geophys. Res.* **2003**, *108* (D12), 4355.

(37) Maria, S. F.; Russell, L. M.; Gilles, M. K.; Myneni, S. C. B. Organic aerosol growth mechanisms and their climate-forcing implications. *Science* **2004**, *306*, 1921−1924.

(38) Croft, B.; Lohmann, U.; von Salzen, K. Black carbon ageing in the Canadian Centre for Climate modelling and analysis atmospheric general circulation model. *Atmos. Chem. Phys.* **2005**, *5*, 1931−1949.

(39) Brubaker, W. W.; Hites, R. A. OH reaction kinetics of polycyclic aromatic hydrocarbons and polychlorinated dibenzo-p-dioxins and dibenzofurans. *J. Phys. Chem. A* **1998**, *102*, 915−921.

(40) U.S. EPA *Estimation Programs Interface Suite for Microsoft Windows, v 4.10*; United States Environmental Protection Agency: Washington, DC, 2011.

(41) Pöschl, U.; Letzel, T.; Schauer, C.; Niessner, R. Interaction of ozone and water vapor with spark discharge soot aerosol particles coated with benzo[a]pyrene: O_3 and H_2O adsorption, benzo[a]pyrene degradation, and atmospheric implications. *J. Phys. Chem. A* **2001**, *105*, 4029−4041.

(42) Kahan, T. F.; Kwamena, N.-O. A.; Donaldson, D. J. Heterogeneous ozonation kinetics of polycyclic aromatic hydrocarbons on organic films. *Atmos. Environ.* **2006**, *40*, 3448−3459.

(43) Kwamena, N.-O. A.; Thornton, J. A.; Abbatt, J. P. D. Kinetics of surface-bound benzo[a]pyrene and ozone on solid organic and salt aerosols. *J. Phys. Chem. A* **2004**, *108*, 11626−11634.

(44) Liu, H.; Jacob, D. J.; Bey, I.; Yantosca, R. M. Constraints from ^{210}Pb and ^{7}Be on wet deposition and transport in a global three-dimensional chemical tracer model driven by assimilated meteorological fields. *J. Geophys. Res.* **2001**, *106* (D11), 12109−12128.

(45) Wania, F.; Mackay, D.; Hoff, J. T. The importance of snow scavenging of polychlorinated biphenyl and polycyclic aromatic hydrocarbon vapors. *Environ. Sci. Technol.* **1999**, *33*, 195−197.

(46) Daly, G. L.; Wania, F. Simulating the influence of snow on the fate of organic compounds. *Environ. Sci. Technol.* **2004**, *38*, 4176−4186.

(47) Wesely, M. L. Parameterization of surface resistances to gaseous dry deposition in regional-scale numerical models. *Atmos. Environ.* **1989**, *23*, 1293−1304.

(48) Wang, Y.; Jacob, D.; Logan, J. Global simulation of tropospheric O_3-NO_x-hydrocarbon chemistry: 1. Model formulation. *J. Geophys. Res.* **1998**, *103* (D9), 10,713−10,725.

(49) Simonich, S. L.; Hites, R. A. Importance of vegetation in removing polycyclic aromatic hydrocarbons from the atmosphere. *Nature* **1994**, *370*, 49−51.

(50) Simonich, S. L.; Hites, R. A. Vegetation-atmosphere partitioning of polycyclic aromatic- hydrocarbons. *Environ. Sci. Technol.* **1994**, *28*, 939−943.

(51) Simonich, S. L.; Hites, R. A. Organic pollutant accumulation in vegetation. *Environ. Sci. Technol.* **1995**, *29*, 2905−2914.

(52) Nizzetto, L.; Lohmann, R.; Gioia, R.; Jahnke, A.; Temme, C.; Dachs, J.; Herckes, P.; Di Guardo, A.; Jones, K. C. PAHs in air and seawater along a North-South Atlantic transect: Trends, processes and possible sources. *Environ. Sci. Technol.* **2008**, *42*, 1580−1585.

(53) Del Vento, S.; Dachs, J. Atmospheric occurrence and deposition of polycyclic aromatic hydrocarbons in the northeast tropical and subtropical Atlantic Ocean. *Environ. Sci. Technol.* **2007**, *41*, 5608−5613.

(54) Meijer, S. N.; Sweetman, A. J.; Halsall, C. J.; Jones, K. C. Temporal trends of polycyclic aromatic hydrocarbons in the UK atmosphere: 1991−2005. *Environ. Sci. Technol.* **2008**, *42*, 3213−3218.

(55) Sun, P.; Backus, S.; Blanchard, P.; Hites, R. A. Annual variation of polycyclic aromatic hydrocarbon concentrations in precipitation collected near the Great Lakes. *Environ. Sci. Technol.* **2006**, *40*, 696−701.

(56) Frossard, A. A.; Shaw, P. M.; Russell, L. M.; Kroll, J. H.; Canagaratna, M. R.; Worsnop, D. R.; Quinn, P. K.; Bates, T. S. Springtime Arctic haze contributions of submicron organic particles

from European and Asian combustion sources. *J. Geophys. Res.* **2011**, *116*, D05205.

(57) Galarneau, E.; Bidleman, T. F.; Blanchard, P. Seasonality and interspecies differences in particle/gas partitioning of PAHs observed by the Integrated Atmospheric Deposition Network (IADN). *Atmos. Environ.* **2006**, *40*, 182−197.

(58) Arp, H. P. H.; Schwarzenbach, R. P.; Goss, K.-U. Ambient gas/particle partitioning. 2: The influence of particle source and temperature on sorption to dry terrestrial aerosols. *Environ. Sci. Technol.* **2008**, *42*, 5951−5957.

(59) Goss, K. U.; Eisenreich, S. J. Sorption of volatile organic compounds to particles from a combustion source at different temperatures and relative humidities. *Atmos. Environ.* **1997**, *31*, 2827−2834.

(60) Eckhardt, S.; Breivik, K.; Manoe, S.; Stohl, A. Record high peaks in PCB concentrations in the Arctic atmosphere due to long-range transport of biomass burning emissions. *Atmos. Chem. Phys.* **2007**, *7*, 4527−4536.

(61) *Co-operative Programme for Monitoring and Evaluation of the Long-range Transmission of Air Pollutants in Europe (EMEP). NO42 Spitsbergen, Zeppelin, Site Description*; http://www.nilu.no/projects/ccc/sitedescriptions/no/index.html.

(62) Chen, Y.; Li, Q.; Randerson, J. T.; Lyons, E. A.; Kahn, R. A.; Nelson, D. L.; Diner, D. J. The sensitivity of CO and aerosol transport to the temporal and vertical distribution of North American boreal fire emissions. *Atmos. Chem. Phys.* **2009**, *9*, 6559−6580.

(63) Turquety, S.; Logan, J. A.; Jacob, D. J.; Hudman, R. C.; Leung, F. Y.; Heald, C. L.; Yantosca, R. M.; Wu, S.; Emmons, L. K.; Edwards, D. P.; Sachse, G. W. Inventory of boreal fire emissions for North America in 2004: Importance of peat burning and pyroconvective injection. *J. Geophys. Res.* **2007**, *112*, D12S03.

(64) Kim, J. Y.; Lee, J. Y.; Choi, S.-D.; Kim, Y. P.; Ghim, Y. S. Gaseous and particulate polycyclic aromatic hydrocarbons at the Gosan background site in East Asia. *Atmos. Environ.* **2012**, *49*, 311−319.

(65) Rodan, B. D.; Pennington, D. W.; Eckley, N.; Boethling, R. S. International action on persistent organic pollutants: Techniques to provide a scientific basis for POPs criteria in international negotiation. *Environ. Sci. Technol.* **1999**, *33*, 3482−2488.

(66) Wang, W.; Massey Simonich, S. L.; Wang, W.; Giri, B.; Zhao, J.; Xue; Cao, J.; Lu, X.; Tao, S. Atmospheric polycyclic aromatic hydrocarbon concentrations and gas/particle partitioning at background, rural village and urban sites in the North China Plain. *Atmos. Res.* **2011**, *99*, 197−206.

MIT JOINT PROGRAM ON THE SCIENCE AND POLICY OF GLOBAL CHANGE
REPRINT SERIES Recent Issues

Joint Program Reprints are available free of charge (limited quantities). To order: please use contact information on inside of front cover.

2011-21 The Role of Growth and Trade in Agricultural Adaptation to Environmental Change, Reilly, J.M., in: *Handbook on Climate Change and Agriculture.* A. Dinar and R. Mendelsohn (Editors), Edward Elgar Publishing: UK and USA, pp. 230–268 (2011)

2011-22 Science and Strategies to Reduce Mercury Risks: A Critical Review, Selin, N.E. *Journal of Environmental Monitoring*, 13(9): 2389–2399 (2011)

2012-1 The Influence of Shale Gas on U.S. Energy and Environmental Policy, Jacoby, H.D., F. O'Sullivan and S. Paltsev, *Economics of Energy and Environmental Policy*, 1(1): 37–51 (2012)

2012-2 Biofuels, Climate Policy, and the European Vehicle Fleet, Gitiaux, X.S., S. Paltsev, J. Reilly and S. Rausch, *Journal of Transport Economics and Policy*, 46(1): 1–23 (2012)

2012-3 Health Damages from Air Pollution in China, Matus, K., K.-M. Nam, N.E. Selin, L.N. Lamsal, J.M. Reilly and S. Paltsev, *Global Environmental Change*, 22(1): 55–66 (2012)

2012-4 Analysis of Climate Policy Targets under Uncertainty, Webster, M.D., A.P Sokolov, J.M. Reilly, C. Forest, S. Paltsev, C.A. Schlosser, C. Wang, D.W. Kicklighter, M. Sarofim, J.M. Melillo, R.G. Prinn and H.D. Jacoby, *Climatic Change*, 112(3-4): 569–583 (2012)

2012-5 The Impact of the European Union Emissions Trading Scheme on U.S. Aviation, Malina, R., D. McConnachie, N. Winchester, C. Wollersheim, S. Paltsev and I. Waitz, *Journal of Air Transport Management*, 19: 36–41 (2012)

2012-6 Interconnection of Nitrogen Fixers and Iron in the Pacific Ocean: Theory and Numerical Simulations, Dutkiewicz, S., B.A. Ward, F.M. Montiero, and M.J. Follows, *Global Biogeochemical Cycles*, 26, GB1012 (2012)

2012-7 The Weak Tie Between Natural Gas and Oil Prices, Ramburg, D.J. and J.E. Parsons, *The Energy Journal*, 33(2): 13–35 (2012)

2012-8 Atmospheric Chemistry, Modeling, and Biogeochemistry of Mercury, Selin, N.E, in: *Mercury in the Environment: Pattern and Process*. M.S. Banks (Editor), University of California Press: Berkeley, U.S., pp. 73–80 (2012)

2012-9 Uncertainty analysis of vegetation distribution in the northern high latitudes during the 21st century with a dynamic vegetation model, Jiang, Y., Q. Zhuang, S. Schaphoff, S. Sitch, A. Sokolov, D. Kicklighter and J. Melillo, *Ecology and Evolution*, 2(3): 593–614 (2012)

2012-10 Impact of aerosols on convective clouds and precipitation, Tao, W., J.-P. Chen, Z. Li, C. Wang, and C. Zhang, *Review of Geophysics*, 50, RG2001, (2012)

2012-11 Using Land to Mitigate Climate Change: Hitting the Target, Recognizing the Trade-Offs, Reilly, J., J. Melillo, Y. Cai, D. Kicklighter, A. Gurgel, S. Paltsev, T. Cronin, A. Sokolov and A. Schlosser, *Environmental Science & Technology*, 46(11): 5672–5679 (2012)

2012-12 Development and application of earth system models, Prinn, R.G., *Proceedings of the National Academy of Sciences*, online first, www.pnas.org/cgi/doi/10.1073/pnas.1107470109 (2012)

2012-13 Emissions Pricing to Stabilize Global Climate, Bosetti, V., S. Paltsev, J. Reilly and C. Carraro, in *Fiscal Policy to Mitigate Climate Change: A Guide for Policymakers*. R. de Mooij, I.W.H. Parry and M. Keen (eds.), International Monetary Fund: Washington, D.C., pp. 49–67 (2012)

2012-14 The Impact of Border Carbon Adjustments Under Alternative Producer Responses, Winchester, N., *American Journal of Agricultural Economics*, 94(2): 354–359 (2012)

2012-15 Long-Range Atmospheric Transport of Polycyclic Aromatic Hydrocarbons: A Global 3-D Model Analysis Including Evaluation of Arctic Sources, Friedman, C.L. and N.E. Selin, *Environmental Science & Technology*, 46(17): 9501–9510 (2012)